Desalination and Water Treatment
www.deswater.com
doi: 10.5004/dwt.2023.29734

300 (2023) 101–106
July

Removal of formaldehyde in water with low concentration of hydrogen peroxide catalyzed by lanthanum-silicon oxide composite

Qingguo Ma*, Siyang Shi, Fengfan Yang, Xuan Zhang

Department of Chemistry and Chemical Engineering, Taiyuan Institute of Technology, Taiyuan 030008, Shanxi Province, China, emails: maqg@tit.edu.cn (Q. Ma), 893941777@qq.com (S. Shi), 1242325087@qq.com (F. Yang), 1786620584@qq.com (X. Zhang)

Received 25 July 2022; Accepted 25 June 2023

ABSTRACT

The wide application of formaldehyde (HCHO) makes it a common pollutant in the environment. HCHO has a destructive effect on the ecological environment. Catalytic oxidation has been widely used in the fields of HCHO wastewater treatment. Lanthanum-silicon oxide composite (La_2O_3-SiO_2) was synthesized by the sol–gel method. The structure of La_2O_3-SiO_2 was characterized by an X-ray diffractometer, X-ray photoelectron spectroscopy, and transmission electron microscopy. The catalytic activity for HCHO oxidation with a low concentration of hydrogen peroxide (H_2O_2, 32–98 mM) over La_2O_3-SiO_2 with different lanthanum oxide (La_2O_3) contents were investigated at room temperature. The results show that the La_2O_3-SiO_2 with 10 wt.% La_2O_3 leads the best catalytic activity and stability. The addition of La_2O_3-SiO_2 significantly enhanced the process of removing HCHO (0.4~3 mg/mL) from the water. As-synthesized La_2O_3-SiO_2 composites facilitate HCHO (0.4~3 mg/mL) removal rate (92.1%–97.3%) within 20 min at room temperature with a low concentration of hydrogen peroxide (85 mM), and it can be readily regenerated at low temperature (80°C). HCOOH is the intermediate species in HCHO oxidation over La_2O_3-SiO_2. The HCHO oxidation mechanism on La_2O_3-SiO_2 is verified.

Keywords: Formaldehyde; Catalytic oxidation; Hydrogen peroxide; Lanthanum oxide; Silica

1. Introduction

Due to the high reactivity of formaldehyde (HCHO), its use in industry has increased. Many industrial products are made from HCHO, such as urea-formaldehyde resin [1], phenol-formaldehyde resin [2], wood adhesive [3], pulp and paper mills [4], cosmetics [5], preservatives [6], fibers [7] and so on. The wide application of HCHO makes it a common pollutant in the environment. HCHO has a destructive effect on the ecological environment. It is carcinogenic and harmful to reproduction, cognitive function, and growth [8–10].

There are many physical, chemical, and biological methods to treat HCHO in wastewater, such as adsorption [11], ultraviolet (UV) [12], light-catalyzed reaction [13], electrochemical process [14], membrane processes [15], catalytic oxidation [16], etc. Among these methods, catalytic oxidation has been widely used in the fields of HCHO wastewater treatment. It has the advantages of fast reactivity, wide application range, and no secondary pollution. Catalytic oxidation can directly convert HCHO into carbon dioxide and water. Photo-Fenton degradation of HCHO is one of the advanced oxidation processes. Different research groups have investigated the treatment of HCHO. For example, Mohammadifard et al. [17] studied the efficiency of MIL-100(Fe) under visible light irradiation toward the degradation of HCHO. Guimaraes [18] used UV/H_2O_2 and photo-Fenton advanced oxidation processes to degrade formaldehyde at the highest concentrations (1,200–12,000 mg/L). The degradation of HCHO was high to 98%.

* Corresponding author.

Although the photo-Fenton process is highly effective in treating HCHO, its pH is limited to a certain range, resulting in the discharge of iron sludge and the use of harmful and expensive UV light [17]. The lanthanum oxide (La_2O_3) material is one of the widely used catalysts for catalytic oxidation. La_2O_3 is used in many applications because of its large bandgap energy of 5.5 eV and high electrical permittivity (K = 27) [19]. Active oxygen sites are formed on La_2O_3 catalysts in catalytic oxidation reactions. It is used in various domains such as phosphate removal [20], removal of toxic organic pollutants [21], optoelectronic applications [19], and catalytic reactions [22–25].

To study the effect of La_2O_3 on the removal of HCHO in wastewater, the lanthanum-silicon oxide (La_2O_3-SiO_2/H_2O_2) system was proposed for the removal of HCHO in sewage. The amount of La_2O_3-SiO_2, and the concentration of H_2O_2 and HCHO on the removal rate of HCHO were investigated. The formation of the intermediate and the possible reaction mechanisms of the degradation of formaldehyde by La_2O_3-SiO_2/H_2O_2 were investigated. La_2O_3-SiO_2 exhibited superior catalytic performance and high stability.

2. Materials and methods

La_2O_3-SiO_2 was synthesized by the sol–gel method. Lanthanum(III) nitrate hexahydrate was dissolved in a mixture of 2.0 mL deionized water, 10.4 g tetraethyl orthosilicate, and 70 mL ethanol. The mixture was stirred and heated at 70°C on a magnetic stirrer until gel formed. The obtained gel product was dried at 80°C for 4 h and then calcined in an air atmosphere for 6 h at 800°C.

The structures of La_2O_3-SiO_2 were characterized by X-ray diffraction (Rigaku, Smartlab, Japan), X-ray photoelectron spectroscopy (XPS; Thermo Fisher, Thermo Scientific K-Alpha, USA), and transmission electron microscopy (TEM). XPS spectra of La_2O_3-SiO_2 were measured on a SPECES Spectrometer equipped with a monochromatic Al Ka source (1,486.6 eV), and the operating pressure was less than 5×10^{-9} mbar. TEM images of the researched composites were recorded on JEM-F200 (Japan) operating at 200 kV.

The actual lanthanum content in the catalyst of La_2O_3-SiO_2 was determined by inductively coupled plasma optical emission spectroscopy. The instrument type is Agilent 5110 (USA).

The catalytic activity and stability of La_2O_3-SiO_2 were researched towards the oxidation of HCHO with H_2O_2 as an oxidant. In a catalytic activity process, under stirring conditions, 0.06 g La_2O_3-SiO_2 was added into a 5 mL solution of HCHO (1.1 mg/mL). Then, 43 µL H_2O_2 (85 mM in the reaction solution) was added to the above mixture solution and was kept at 25°C for 10 min. After that, the reaction mixture was transferred to the centrifuge tube and centrifuged for 10 min to remove La_2O_3-SiO_2, and then 0.07 g sodium thiosulfate was added to remove the excess H_2O_2.

Although HCHO cannot be detected by diode array detector (DAD) of high-performance liquid chromatography (HPLC), HCHO can react with 2,4-dinitrophenylhydrazine in the presence of sodium acetate buffer solution to produce 2,4-dinitrophenylhydrazone, has a maximum absorption wavelength of 365 nm. So, the conversion of HCHO was calculated by determining 2,4-dinitrophenylhydrazone in the reaction mixture by the standard curve method. The reaction conditions of HCHO and 2,4-dinitrophenylhydrazine are as follows: 100 ul of HCHO solution after the oxidation was transferred to a 10 mL volumetric flask, 1 mL 2,4-dinitrophenylhydrazine solution and 1 mL sodium acetate buffer solution were added, and then methanol was added to 10 mL. Transfer the volumetric flask to a water bath and react at 60°C for 30 min. The product of 2,4-dinitrophenylhydrazone was detected by an UltiMate 3000 HPLC (USA) with DAD. Column: SinoChrom ODS-C18 5 um 4.6*200 mm, column temperature: 30°C, mobile phase: v(methanol)/v(water) = (65/35), flow rate: 1 mL/min, detection wavelength: 365 nm.

The removal rate of HCHO was calculated according to:

$$\text{Removal rate of HCHO} = \frac{C_0 - C_t}{C_0} \times 100\%$$

where C_0 is the concentrations (mg/mL) of HCHO in initial solution and C_t is the concentrations (mg/mL) of HCHO after reaction.

3. Results

3.1. Sample characterization

Fig. 1 shows the X-ray diffraction patterns of La_2O_3-SiO_2 with different content of La_2O_3. The results reveal that the intensity of the diffraction peak of La_2O_3-SiO_2 is related to the content of La_2O_3.

XPS of the catalyst (La_2O_3-SiO_2) before and after formaldehyde removal is shown in Fig. 2. The peaks at 856.28 and 852.88 eV are assigned to $La3d_{3/2}$, the peaks at 839.28 and 835.98 eV are assigned to $La3d_{5/2}$. The binding energy of $La3d_{3/2}$, and $La3d_{5/2}$ was not changed during the oxidation reaction. The binding energy of Si2p (102.98 eV) and O1s (532.38 eV) was also not changed during the oxidation reaction.

The microstructure of the samples was revealed in detail by TEM analysis. Fig. 3 shows the TEM images of La_2O_3-SiO_2

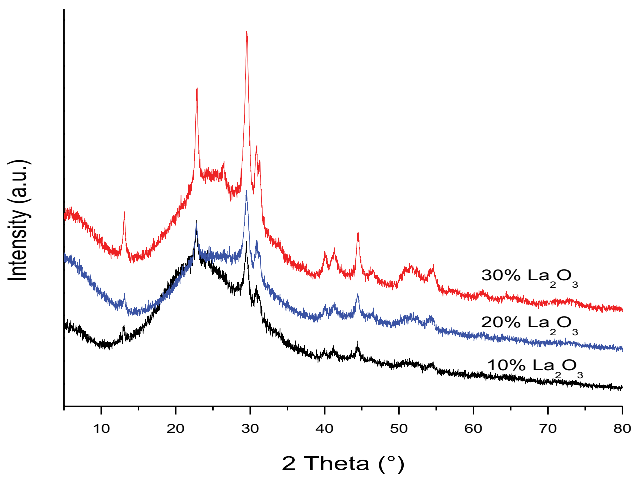

Fig. 1. X-ray diffraction patterns of La_2O_3-SiO_2 with different content of La_2O_3.

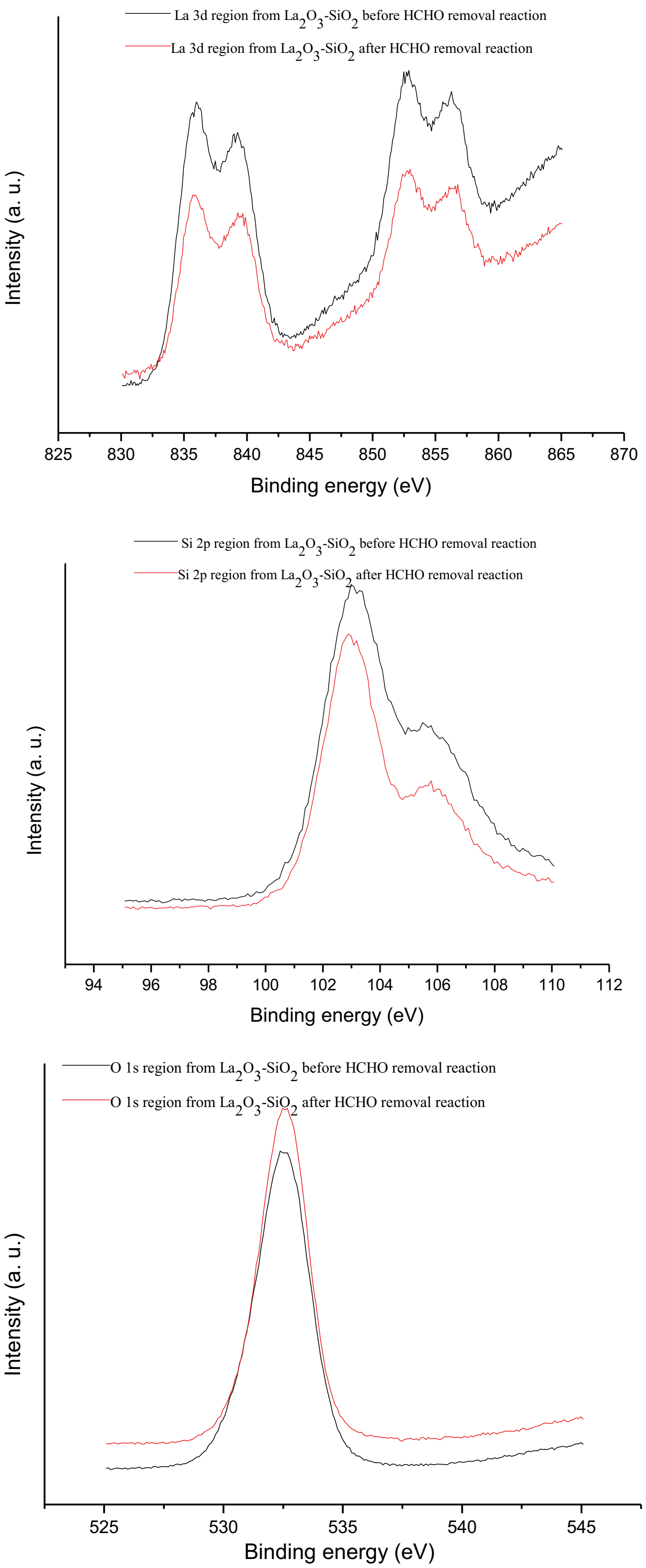

Fig. 2. X-ray photoelectron spectra of La3d, Si2p and O1s region from La_2O_3-SiO_2 before and after HCHO removal reaction.

doped with different contents of La_2O_3. The dispersion of La_2O_3 in the La_2O_3-SiO_2 composite is related to the content of La_2O_3. When the content of La in La_2O_3-SiO_2 is 8.53%, the spacing between La_2O_3 grains is larger. With the increase of La_2O_3 doping, lots of tiny La_2O_3 particles get together. The grain contact is so close that the grain boundary is connected into a piece. The high-resolution TEM from Fig. 3d (inset) confirm that the interlinear spacing of La_2O_3 is 0.234 nm.

3.2. Calibration curve of HCHO

Fig. 4 shows the calibration curve of HCHO. The HCHO concentration of the solution ranges from 0.11 to 11 mg/L. The experimental data are close to the fitting function.

3.3. Influence of the content of La on La_2O_3-SiO_2 for HCHO oxidation

The influence of the content of La on La_2O_3-SiO_2 for HCHO oxidation was investigated. As shown in Table 1 (Entry 2–4), when the content of La is 8.53 wt.%, the removal rate of HCHO is 76.1% at 25°C while it increases to 79.2% over the content of La is 25.58 wt.%. The catalytic activity does not change obviously. The removal rate of HCHO using 8.53 wt.% La of La_2O_3-SiO_2 as a catalyst is higher than that of La_2O_3, indicating that La_2O_3-SiO_2 has higher HCHO catalytic oxidation activity than La_2O_3. To reduce the amount of La in the reaction mixture, the content of La on La_2O_3-SiO_2 is adjusted to a low level of 6.56 wt.%.

As the amount of La_2O_3-SiO_2 increases, the removal rate of HCHO reaches as high as 94.1% at 25°C. As shown in Table 1 (Entry 6–10), when the removal rate of HCHO goes 93.8% at 25°C on La_2O_3-SiO_2, with further addition of La_2O_3-SiO_2 to 0.3g, the increase of HCHO conversion is low. As a result, the optimum amount of La_2O_3-SiO_2 for HCHO oxidation was 0.2 g.

The cyclic stability of La_2O_3-SiO_2 is also studied. La_2O_3-SiO_2 is repeatedly isolated by centrifuge, washed with deionized water, dried at 80°C for 4 h, and used again in the reaction. As presented in Table 1 (Entry 11–13), it exhibits excellent stability in HCHO oxidation where the removal rate of HCHO keep above 90% in three cycle tests.

3.4. Influence of H_2O_2 concentration on the removal rate of HCHO

The influence of H_2O_2 concentration on the removal rate of HCHO over La_2O_3-SiO_2 was studied. As shown in Table 2 (Entry 1–5), under the same reaction condition, improving H_2O_2 concentration (32–98 mM) could enhance the degradation efficiencies of HCHO. When H_2O_2 concentration was greater than 85 mM, the degradation of HCHO does not change obviously. As shown in Table 2 (Entry 4, 6–10), the removal rate of HCHO was accompanied by an extension of the reaction time. However, when the removal rate of HCHO increased to 93.8%, the HCHO degradation did not change obviously with the extension of the reaction time. Because when the concentration of HCHO decreases, the formaldehyde molecule contact with H_2O_2 and La_2O_3-SiO_2 declines.

3.5. Influence of HCHO concentration on the removal rate of HCHO

The change of HCHO concentration in the range of 0.4~3.0 mg/mL was studied in Table 3. It should be noted

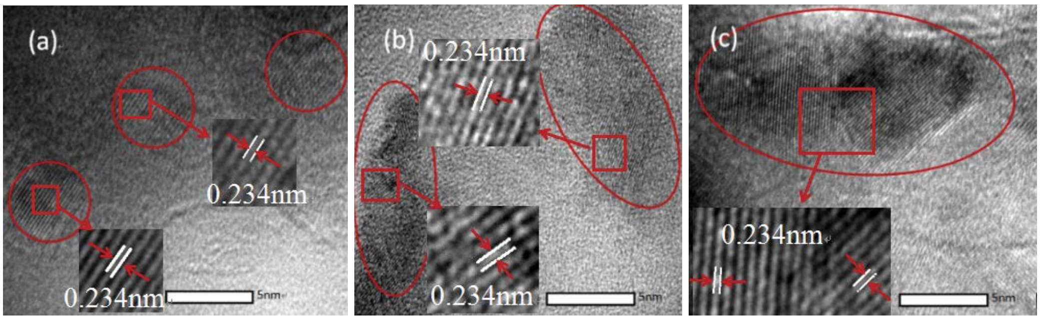

Fig. 3. Transmission electron microscopy images of La_2O_3-SiO_2 doped with different contents of La: (a) 8.53% La_2O_3, (b) 17.05% La_2O_3, and (c) 25.58% La_2O_3.

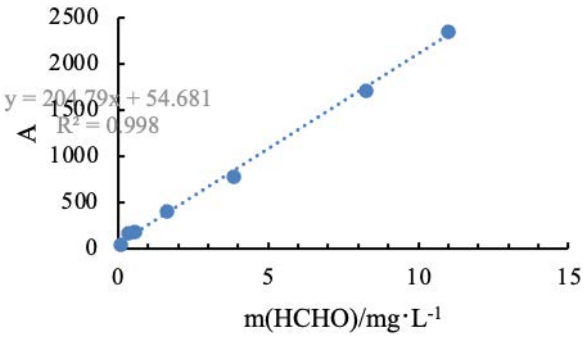

Fig. 4. Calibration curve of HCHO.

Table 1
Catalytic activity of La_2O_3-SiO_2 on the removal rate of HCHO[a]

Entry	Content of La (%)	Amount of La_2O_3-SiO_2 (g)	Removal rate of HCHO (%)
1[b]	–	–	55.1
2	25.58	0.06	79.2
3	17.05	0.06	77.8
4	8.53 (6.56[h])	0.06	76.1
5[c]	–	–	66.1
6	6.56	0.1	82.4
7	6.56	0.15	88.3
8	6.56	0.2	93.8
9	6.56	0.25	94.0
10	6.56	0.3	94.1
11[d]	–	–	56.5
12[e]	6.56	0.2	92.5
13[f]	6.56	0.2	91.3
14[g]	6.56	0.2	90.1

[a]5 mL (1.1 mg/mL) HCHO, H_2O_2 (85 mM), 25°C for 10 min;
[b]without catalyst;
[c]0.01 g La_2O_3 and 0.05 g SiO_2;
[d]0.2 g SiO_2;
[e]first recycled;
[f]second recycled;
[g]third recycled;
[h]actual La content determined by inductively coupled plasma optical emission spectroscopy.

Table 2
Influence of H_2O_2 concentration and time on the removal rate HCHO[a]

Entry	H_2O_2 concentration (mM)	Time (min)	Removal rate of HCHO (%)
1	32	10	66.1
2	48	10	74.2
3	64	10	85.7
4	85	10	93.8
5	98	10	94.5
6	85	2	51.3
7	85	5	85.8
8	85	20	95.9
9	85	30	97.8
10	85	40	97.7

[a]5 mL (1.1 mg/mL) HCHO, La_2O_3-SiO_2 (0.2 g), 25°C.

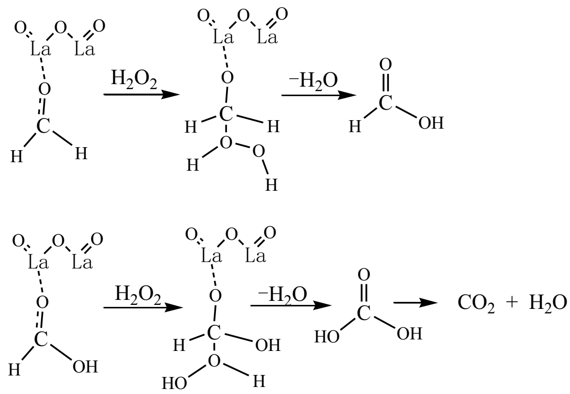

Fig. 5. A possible reaction process for removing HCHO with H_2O_2 over La_2O_3-SiO_2.

that the removal rate of HCHO is higher than 95% when the concentration is higher than 1.1 mg/mL. The removal rate of HCHO decreased as decreasing the HCHO concentration, because when the concentration of HCHO is low, it was hard to continue to react with H_2O_2 over La_2O_3-SiO_2. Compared with La_2O_3-SiO_2, using MIL-100(Fe) as a catalyst, the degradation of HCHO (0.7 mg/mL) is 93% at optimum

Table 3
Influence of the concentration of HCHO on the removal rate of HCHO[a]

Entry	Concentration of HCHO (mg/mL)	Removal rate of HCHO (%)	Yield of HCOOH (%)	HCHO mineralization (%)
1	0.4	91.5	40.5	51.0
2	0.6	92.8	43.5	49.3
3	0.8	95.3	40.3	55.0
4	1.1	95.6	33.4	62.2
5	1.5	96.8	22.4	74.4
6	2.0	97.1	18.6	78.5
7	2.5	97.3	17.8	79.5
8	3.0	97.3	17.9	79.4
9	5.0	97.8	18.7	79.1
10	7.0	97.9	18.5.	79.4
11	10.0	98.8	19.7	79.1

[a]5 mL (0.4–10.0 mg/mL) HCHO, the molar ratio of hydrogen peroxide and formaldehyde is 2.5, La_2O_3-SiO_2 (0.2 g), 25°C for 20 min.

conditions, and the reaction time was lengthy (119 min) [17]. The degradation of HCHO (2.2 mg/mL) was 99.85% at pH 14.0 after 60 min in a rotating packed bed with MgO or MgO/Al_2O_3 as a catalyst, and O_3/H_2O_2 as oxidant [16,26]. In comparison to the above methods, the removal rate of HCHO (0.4 mg/mL) to achieve 90% in the photo-Fenton process (UV/Fe^{2+}/H_2O_2) was instantaneous, this process was performed at pH 3.0 with UV radiation, and the catalyst ($FeSO_4$) cannot be recycled [18]. In this study, La_2O_3-SiO_2 was used as a catalyst, H_2O_2 was used as an oxidant, and no other additives were added, it only takes 20 min, and the removal rate of HCHO is higher than 97% when the concentration is higher than 2.0 mg/mL.

4. Discussion

The oxidation of HCHO is not by hydroxyl radicals. It was verified by the addition of quenchers (hydroquinone, ammonium oxalate, and isopropanol). 0.06 g hydroquinone, ammonium oxalate, or isopropanol, 43 ul of aqueous hydrogen peroxide (30%), 0.2 g La_2O_3-SiO_2 was added into the HCHO standard solution reacted for 10 min at 25°C, the degradation rates of HCHO were 92.9%, 94.5% and 93.4%, respectively. The addition of the quenchers has little effect on the degradation rate of HCHO. In addition, the concentration of hydrogen peroxide did not change with the addition of La_2O_3-SiO_2. 0.2 g La_2O_3-SiO_2 was added into 5 mL aqueous hydrogen peroxide (30%) and react for 10 min at 25°C with stirring. The concentration of hydrogen peroxide after the reaction was the same as the initial solution (9.9 mol/L).

The role of La_2O_3 is as an electron capture center. La undergoes coordination interactions with lone electron pairs of various Lewis bases [27,28]. The superior catalytic performance for removing HCHO with La_2O_3-SiO_2 indicates the possible reaction process, and it is shown in Fig. 5. Firstly, the carbonyl group of HCHO was coordinated to the lanthanum center of La_2O_3-SiO_2, and the density of electrons around carbon atoms decreased. Subsequently, the H_2O_2 reacts with electrophilic C of the carbonyl group. After the deprivation of H_2O, HCHO is replaced by HCOOH [18]. Following this reaction, the carbonyl group of HCOOH was coordinated to the lanthanum center of La_2O_3-SiO_2, and then the H_2O_2 reacted with electrophilic C of the carbonyl group. Finally, CO_2 is formed. The formation of HCOOH as an intermediate is determined by comparing it with the formic acid standard using HPLC. The appearance of CO_2 was approved by the lime water test.

5. Conclusions

The synthesized La_2O_3-SiO_2 exhibited superior catalytic performance and high stability toward the degradation of HCHO with H_2O_2 as an oxidant. The result showed that La_2O_3-SiO_2 effectively degraded HCHO above 92% to CO_2. Its catalytic activity is much higher than the single La_2O_3. The optimum conditions for removal of HCHO (5 mL 1.1 mg/mL) with La_2O_3-SiO_2 as a catalyst, the amount of La_2O_3-SiO_2 was 0.2 g, H_2O_2 concentration was 85 mM, and the reaction time was 20 min. The high catalytic activity, excellent reusability, and better reproducibility of La_2O_3-SiO_2 make it a promising catalyst for the removal of HCHO pollutants in a clearing environment.

Funding

This research was funded by Scientific and Technological Innovation Programs of Higher Education Institutions in Shanxi, grant number 2019L0919. This work was also supported by the Fund for Shanxi "1331 Project" and the National Natural Science Fund of China (Grant number 22072105).

References

[1] H. Pu, K. Han, R. Dai, Z. Shan, Semi-liquefied bamboo modified urea-formaldehyde resin to synthesize composite adhesives, Int. J. Adhes. Adhes., 113 (2022) 103061, doi: 10.1016/j.ijadhadh.2021.103061.

[2] S. Manna, P. Bobde, D. Roy, A.K. Sharma, S.J. Mondal, Separation of iodine using neem oil-cashew nut shell liquid based-phenol formaldehyde resin modified lignocellulosic biomatrices: batch and column study, J. Taiwan Inst. Chem. Eng., 122 (2021) 98–105.

[3] R. Zhang, X. Jin, X. Wen, Q. Chen, D. Qin, Alumina nanoparticle modified phenol-formaldehyde resin as a wood adhesive, Int. J. Adhes. Adhes., 81 (2018) 79–82.
[4] X. Tong, W. Shen, X. Chen, J. Corriou, Qualitative and quantitative analysis of gaseous pollutants for cleaner production in pulp and paper mills, J. Cleaner Prod., 9 (2018) 1066–1075.
[5] P. Miralles, A. Chisvert, M.A. Sandra, H.A. Salvador, Determination of free formaldehyde in cosmetics containing formaldehyde-releasing preservatives by reversed-phase dispersive liquid–liquid microextraction and liquid chromatography with post-column derivatization, J. Chromatogr. A, 1543 (2018) 34–39.
[6] K. Sang-Tae, K. Winkowski, M. Tallon, F. Wu, M. Bogers, C. Choi, J. Kupny, In-use consumer safety of formaldehyde-donor preservatives used in personal care products, Toxicol. Lett., 280S (2017) S191–S194.
[7] E. Keijsers, M.V.D. Oever, J.V. Dam, A. Lansbergen, C. Koning, H.V.D. Akker, The development of reed composite fiberboards using partially bio-based, formaldehyde and monomeric isocyanate-free resins, Reinf. Plast., 64 (2020) 195–203.
[8] Y. Kou, H. Zhao, D. Cui, H. Han, Z. Tong, Formaldehyde toxicity in age-related neurological dementia, Ageing Res. Rev., 73 (2022) 101512, doi: 10.1016/j.arr.2021.101512.
[9] A. Duong, C. Steinmaus, C.M. McHale, C.P. Vaughan, L. Zhang, Reproductive and developmental toxicity of formaldehyde: a systematic review, Mutat. Res. Rev. Mutat. Res., 728 (2011) 118–138.
[10] T. Li, F. Chen, Q. Zhou, X. Wang, C. Liao, L. Zhou, L. Wan, J. An, Y. Wan, N. Li, Unignorable toxicity of formaldehyde on electroactive bacteria in bioelectrochemical systems, Environ. Res., 183 (2020) 109143, doi: 10.1016/j.envres.2020.109143.
[11] M. Wang, B. Wen, B. Fan, H. Zhang, Study on adsorption mechanism of silicate adsorbents with different morphologies and pore structures towards formaldehyde in water, Colloids Surf., A, 599 (2020) 124887, doi: 10.1016/j.colsurfa.2020.124887.
[12] A. Talaiekhozani, M. Salari, M.R. Talaei, M. Bagheri, Z. Eskandari, Formaldehyde removal from wastewater and air by using UV, ferrate(VI) and UV/ferrate(VI), J. Environ. Manage., 184 (2016) 204–209.
[13] Y. Tan, C. Yin, S. Zheng, Y. Di, Z. Sun, C. Li, Design and controllable preparation of Bi_2MoO_6/attapulgite photocatalyst for the removal of tetracycline and formaldehyde, Appl. Clay Sci., 215 (2021) 106319, doi: 10.1016/j.clay.2021.106319.
[14] D. Yuan, L. Tian, D. Gu, X. Shen, L. Zhu, H. Wu, B. Wang, Fast and efficient oxidation of formaldehyde in wastewater via the solar thermal electrochemical process tuned by thermo-electrochemistry, J. Cleaner Prod., 156 (2017) 310–316.
[15] F.E. Titchou, H. Zazou, H. Afanga, J.E. Gaayda, R.A. Akbour, P.V. Nidheesh, M. Hamdani, Removal of organic pollutants from wastewater by advanced oxidation processes and its combination with membrane processes, Chem. Eng. Process. Process Intensif., 169 (2021) 108631, doi: 10.1016/j.cep.2021.108631.
[16] L. Du, W. Gao, Z. Li, W. Jiao, Y. Liu, Oxidative degradation of formaldehyde in wastewater by $MgO/O_3/H_2O_2$ in a rotating packed bed, Chem. Eng. Process. Process Intensif., 155 (2020) 108053, doi: 10.1016/j.cep.2020.108053.
[17] Z. Mohammadifard, R. Saboori, N.S. Mirbagheri, S. Sabbaghi, Heterogeneous photo-Fenton degradation of formaldehyde using MIL-100(Fe) under visible light irradiation, Environ. Pollut., 251 (2019) 783–791.
[18] J.R. Guimaraes, C.R.T. Farah, M.G. Maniero, P.S. Fadini, Degradation of formaldehyde by advanced oxidation processes, J. Environ. Manage., 107 (2012) 96–101.
[19] R. Jbeli, A. Mami, C. Bilel, F. Saadallah, M. Bouaicha, M. Amlouk, Growth and investigation of $LaNiO_3/La_2O_3$ composites films for optoelectronic applications, Optik, 247 (2021) 168013, doi: 10.1016/j.ijleo.2021.168013.
[20] Y. Chang, Z. Wei, X. Chang, G. Ma, L. Meng, T. Liu, L. Yang, Y. Guo, X. Ma, Hollow hierarchically porous La_2O_3 with controllable multishells: a high-performance adsorbent for phosphate removal, Chem. Eng. J., 421 (2021) 127816, doi: 10.1016/j.cej.2020.127816.
[21] T. Abraham, R.N. Priyanka, S. Joseph, A.R. Chacko, B. Mathew, Fabrication of La_2O_3/Bi_2O_3/silver orthophosphate heterojunction catalyst for the visible light mediated remediation of refractory pollutants, Mater. Res. Bull., 140 (2021) 111299, doi: 10.1016/j.materresbull.2021.111299.
[22] Y. Li, P. Niu, Q. Wang, L. Jia, M. Lin, D. Li. Performance of Zn-Al co-doped La_2O_3 catalysts in the oxidative coupling of methane catalysts in the oxidative coupling of methane, J. Fuel Chem. Technol., 49 (2021) 1458–1467.
[23] C. Huang, Y. Yu, J. Yang, Y. Yan, D. Wang, F. Hu, X. Wang, R. Zhang, G. Feng, Ru/La_2O_3 catalyst for ammonia decomposition to hydrogen, Appl. Surf. Sci., 476 (2019) 928–936.
[24] G. Sharma, A. Kumar, S. Sharma, S.I. Al-Saeedi, G.M. Al-Senani, A. Nafady, T. Ahamad, M. Naushad, F.J. Stadler, Fabrication of oxidized graphite supported La_2O_3/ZrO_2 nanocomposite for the photoremediation of toxic fast green dye, J. Mol. Liq., 277 (2019) 738–748.
[25] Y. Xie, J. Wu, C. Sun, Y. Ling, S. Li, X. Li, J. Zhao, K. Yang, La_2O_3-modified graphite carbon nitride achieving the enhanced photocatalytic degradation of different organic pollutants under visible light irradiation, Mater. Chem. Phys., 246 (2020) 122846, doi: 10.1016/j.matchemphys.2020.122846.
[26] L. Du, P. Li, W. Gao; X. Ding, W. Jiao, Y. Liu, Enhancement degradation of formaldehyde by $MgO/\gamma\text{-}Al_2O_3$ catalyzed O_3/H_2O_2 in a rotating packed bed, J. Taiwan Inst. Chem. Eng., 118 (2021) 29–37.
[27] H.R. Li, B. Feng, Visible-light-driven composite La_2O_3/TiO_2 nanotube arrays: synthesis and improved photocatalytic activity, Mater. Sci. Semicond. Process., 43 (2016) 55–59.
[28] Y. Cong, B. Tian, J. Zhan, Improving the thermal stability and photocatalytic activity of nanosized titanium dioxide via La^{3+} and N co-doping, Appl. Catal., B, 101 (2011) 376–381.